Evaluation of the Electromagnetic Environment Around Underground HVDC Lines

Luca Zilberti, Enrico Pons, Oriano Bottauscio, Mario Chiampi, and Michele Pastorelli

Abstract—This paper analyses the magnetic-field emissions of a high-voltage dc transmission line constituted by two couples of underground cables laid along a highway. The transmission system, including all its components (transformers, converters filters, and line), is modeled through a circuital approach, which provides the distribution of the current harmonics along the line length. The magnetic field produced in the environment is then estimated by a hybrid finite element/boundary element method. The electromagnetic interferences with existing appliances and the human exposure to magnetic fields are investigated considering different laying configurations, conductor dispositions, and supply conditions. Compliance with regulations limiting human exposure and technical standards ensuring electromagnetic compatibility of appliances and devices are assessed.

Index Terms—Electromagnetic compatibility, electromagnetic fields, high-voltage direct-current (HVDC) transmission lines, modeling, power transmission.

I. INTRODUCTION

HIGH-VOLTAGE direct-current (HVDC) technology has had rapid development as an alternative to the conventional power transmission lines. For economic and technical reasons, HVDC connections are widely applied in high-power transmission over long distances and power transmission through submarine cables and interconnection of ac systems asynchronous or with different frequencies. Additional advantages are slight disturbances to telephone wires and reduced voltage drop along the lines. The higher initial costs of the conversion plants are compensated by the reduced operating costs due to lower losses.

Other important factors, which must be evaluated for a correct choice between HVDC and HVAC systems, are related to the specific economic and social situations of the sites where the lines must be installed. For example, social and political reasons can lead to prefer HVDC links in highly populated areas or in touristic sites, thanks to the possibility of utilizing underground cables in place of overhead lines. Moreover, in these cases, pre-existing structures (e.g., highways and tunnels) can be employed for the cable laying, reducing the environmental impact.

TABLE I
ICNIRP MAGNETIC-FIELD REFERENCE LEVELS (A/m)

Frequency (f)	General public exposure	Occupational exposure
Static field	$3.2 \cdot 10^5$	$1.6 \cdot 10^6$
up to 1 Hz	$3.2 \cdot 10^4$	$1.63 \cdot 10^5$
0.025 – 0.82 kHz	-	$20/f$
0.025 – 0.8 kHz	$4/f$	-
0.82 – 65 kHz	-	24.4
0.8 – 3 kHz	5	-

Different from submarine cables, underground HVDC cables can interfere with people, installation, and equipment and must comply with the limits for human exposure [1]–[4] and with the standards ensuring electromagnetic compatibility (EMC) of vehicles and technological services [5]. In fact, EMC interference could arise from the presence of harmonics components superimposed to the dc current and generated by ac/dc and dc/ac conversion plants [6]–[11].

This paper evaluates the electromagnetic emission of HVDC underground lines and discusses their effects, making reference to the design data of two HV cable lines that will interconnect Italy and France via the Frejus tunnel. This paper has been carried out in the framework of the research project "Transmission Infrastructure for Power Exchange (TIPE)" supported by the Regione Piemonte (Italy). The study starts from the analysis of the ICNIRP magnetic-field limits for general public and workers and EMC reference levels for different appliances, as reported in Section II. The impact on the environment is evaluated through a modeling approach, which combines three steps: 1) electromagnetic and electrostatic field solutions to evaluate the line parameters (inductances and capacitance); 2) a circuital approach which includes the line and the source/user converters providing the current harmonic distribution along the line; and 3) an electromagnetic-field solution to obtain the magnetic field around a chosen point of the line, also including the possible presence of magnetic and conductive shields. All of the models are described in Section III. The proposed approach is applied to the designed underground line whose characteristics are presented in Section IV, together with the considered supply conditions. The spatial waveform of the current harmonic components along the line are computed and discussed in Section V. Finally, the magnetic-field distribution around the HVDC cables is presented in Section VI, where the solutions for complying with the reference levels are also envisaged.

II. ICNIRP AND EMC REFERENCE MAGNETIC-FIELD LEVELS

The magnetic field generated by the new plant must comply with the reference levels introduced to limit human exposure

TABLE II
TYPE OF APPLIANCES CONSIDERED FOR EMC EVALUATIONS

Type of appliance	Reference field (A/m) at 50/60 Hz			Technical Standard
Gas detectors	3			EN 50270:2006-11 [14]
VDU terminals	0.4 (residential/office)	2.4 (commercial/light industrial)	8 (heavy industrial)	ECMA-237 [15]
Fire detectors and cameras	Immunity levels are provided only for radiofrequency fields			EN 50130-4 [16]
Road traffic signal systems	60			EN 50293 [17]
UPS	10 (direct connection to public supply)	30 (non-direct connection to public supply)		EN 62040-2:2006-03 [18]
Residential, commercial and light industrial environments	3			EN 61000-6-1 [5]
Heavy industrial environments	30			EN 61000-6-2 [5]
Information technology equipment	1			EN 55024:1998-09 [19]

and the EMC of the appliances that are usually present in highway infrastructures.

Limits for human exposure are provided by the International Commission on Non-Ionizing Radiation Protection (ICNIRP) Guidelines [1], [2], which establish reference levels for the dc and ac magnetic field (Table I), with the aim of limiting short-term effects. These limits have been adopted in Europe by the 1999/519/EC Council Recommendation for the exposure of general public [3] and by the Directive 2004/40/EC of the European Parliament for the exposure of workers [4] even if, at the moment, the application of this last directive has been postponed. Moreover, recent Italian laws [12], [13] introduced quality targets for new power frequency electric installations in terms of magnetic flux density levels (3 μT, equivalent to a magnetic field of 2.4 A/m). This law, with the consequent low magnetic-field limit, is based on the concept of prudent avoidance, adopted as part of the policy in many countries with the aim of limiting potential long-term effects.

The reference values for EMC evaluations are deduced from the available technical standards. The appliances here considered are listed in Table II and include all of the communications, detections, and security systems usually employed in the highway environment. In all cases, the standards provide reference levels only for 50–60 Hz or radio-frequency fields. In the considered application, the currents include higher order harmonics with respect to the fundamental one of the ac supplies (50 Hz). Thus, taking into account that the effects induced on appliances and plants are proportional to the frequency f, it seems reasonable to scale the 50-Hz limits by a factor $50/f$.

III. MODELING APPROACH

The modeling analysis of the HVDC transmission system constituted by two couples of underground cables can be split into three steps: 1) a preliminary evaluation of the line electric and magnetic parameters, 2) the computation of the current harmonics produced by the converter and of their propagation along the line, and 3) the evaluation of the magnetic field around the cables. Each step will be separately described in the following subsections.

A. Computation of the Line Parameters

The per-unit length inductances and capacitances can be evaluated from electromagnetic and electrostatic-field solutions, re-

spectively. In both cases, the prevailing length of the cables with respect to the other dimensions makes a 2-D approach possible. In addition, the open boundary-domain characteristics suggest the use of a hybrid finite-element method (FEM)—boundary element method (BEM). The whole space is divided into a BEM homogeneous region filled by air, which extends to infinite, and an FEM subdomain, which includes the field sources and any possible body with different properties. The link between FEM and BEM relations is obtained by imposing suitable interface conditions on the closed line separating the two subdomains.

The 2-D electromagnetic problem in the FE region is formulated in terms of a vector potential, taking into account the presence of possible ferromagnetic/conductive layers used for mechanical protection. The BEM equations are deduced by the application of Green's vector theorem to the magnetic field. The per-unit length self inductances of each line and mutual inductance between them are then evaluated from the linked fluxes, following the procedure proposed in [20].

The electric-field distribution is obtained by solving a boundary value problem expressed in terms of an electric scalar potential, where the field sources are the known potentials of each conductive body. The capacitance matrix is then evaluated by computing the electric flux from each conductor, as detailed in [21]. However, in the considered system, the presence of a grounded metallic screen around each single conductor makes the capacitive coupling between different cables negligible. Similar considerations also apply for the mutual conductance.

B. System Model

The whole system includes the supply side (transformers, controlled rectifiers, smoothing reactor), the transmission line composed of two paralleled couples of cables, and the user side (smoothing reactor, controlled rectifiers, transformers).

The supply three-phase voltage systems, on both sides of HVDC line, are connected to the conversion units by single input—double output transformers, to obtaint the required 30° phase shift for the 12 pulses converters. Mutual coupling among all of the transformer windings has been taken into account.

A smoothing reactor has been considered on each line terminal. The SCRs in the converters have been considered with proper series parameters (threshold voltage and equivalent resistance) and without any commutation conditioning circuits (i.e., snubber network).

In steady-state conditions, equal firing angles have been considered for the ac/dc (and dc/ac) bridges; this assumption gives rise to distorted current waveforms which only contains harmonics of order $12n$ with respect to the primary supply frequency (50 Hz) in the case of the symmetrical supply. The second-order harmonic arises when nonsymmetric supply voltages are imposed.

In the employed procedure, the vectors of three-phase voltages at the supply and user sides are imposed, and the model provides the values of the current harmonics at the dc cable terminals and its distribution along the line. Nonsymmetric behavior can be taken into account by adding negative sequences to the voltage vectors.

The lines have been modeled by distributed parameters (per-unit-length longitudinal resistance and inductance r, l and transversal conductance and capacitance g, c), accounting for the inductive coupling between conductors. The values of the cable resistance and inner inductance have been considered equal to the dc values. This carries to a slight overestimation of the harmonic currents; the value of the inner inductance is much lower than the value of the outer inductance; thus, its variation can be disregarded.

The computation of the harmonic content of the dc line current has been carried out in steady-state conditions, evaluating several and realistic sets of ac voltages on both sides of the HVDC system and power transferred by the dc lines. The sets of parameters that produce the higher values of harmonic components have been considered for the computation of the magnetic fields in the surrounding environment.

C. Magnetic-Field Computation

The magnetic field generated by the dc and harmonic components of the current is evaluated by a hybrid FEM–BEM technique, based on the thin-shell formulation [22]. This technique enables the analysis of the magnetic field generated by strand conductors also in the presence of possible magnetic/conducting shield elements (see Appendix A). The computation is performed by just considering the conductive core of the cables. The grounded metallic screens of any single cable are disregarded since preliminary analysis proved that they do not significantly affect the magnetic field in the surrounding region.

In all of the simulations reported here , the harmonics of the two parallel dc lines are assumed to be in phase. This choice has been intentionally assumed in order to consider the most critical conditions. However, if both lines are active, the transmitted power is shared one half per line; this implies that the converters are controlled with the same delay angle with the current harmonics in phase.

IV. FEATURES OF THE ANALYZED SYSTEM

The HVDC transmission system considered here is constituted by two couples of underground HV conductors (lines A and B), which can be separately managed with the only constraint that the power-flow direction is the same for both lines. Each line (A and B) is a bipolar HVDC system supplied by its own transformers that are parallel connected to the three-phase
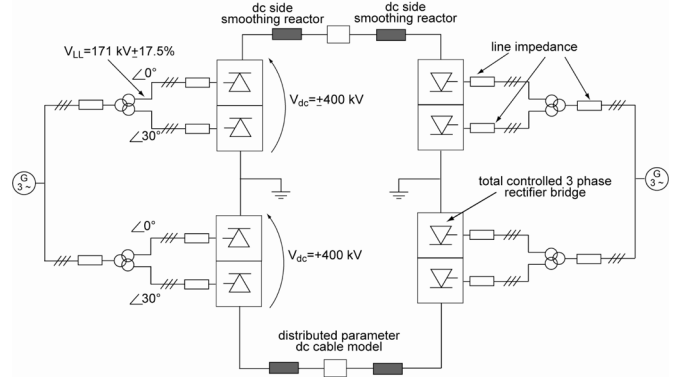

Fig. 1. Model of the analyzed HVDC system (line A or B).

TABLE III
DESIGN VALUES OF A SINGLE HVDC LINE

HVDC line	Rated voltage: ± 400kV
	Rated power: 500 MW
	Rated DC Current: 625 A
	Length: 184 km
Single phase double secondary transformers (three per pole)	Rated power: 100/50/50 MVA
	Rated voltage: 231 kV (YN) / 99.1 kV (Y) / 171.7 kV (Δ)
	Short circuit voltage: 12%
Smoothing reactor (one per cable terminal)	L = 400 mH, R = 0.74 Ω

system (see Fig. 1). Each converter unit consists of two series-connected 12-pulses ac/dc converters. The features of each single line of the HVDC system are presented in Table III.

The two lines can be arranged in different laying configurations, depending on the features of the artifacts (highway, viaduct, tunnel), where the cables are posed (see Table IV). In the main laying (#1), along the highway, the conductors are placed in a horizontal plane below a ferromagnetic sheet used for mechanical protection; along the viaducts (#2) the two lines are posed on brackets which do not affect the electromagnetic behavior; in the tunnels (#3) the conductors are again on a horizontal plane, within a concrete tube. For each laying configuration, two dispositions of the line conductors can be envisaged as presented in Table V. Obviously, the line parameters, in particular the per-unit length self and mutual inductances, depend on the laying configuration, while, for a given laying, the conductor disposition modifies only the sign of the mutual inductance.

Different operating conditions can be found in actual plants. Examples of harmonics measured in an HVDC conversion substation are reported in [23]. The presence of noncanonical harmonics depends on many quantities, whose values can be reasonably limited in a range around their rated value: input/output voltage amplitude of the ac systems (from 90% to 110%), the presence of negative sequences in the voltage vectors (up to 2% of the corresponding positive-sequence voltage at the generator side), transmitted power (from 80% to 100%), and current sharing between the two parallel lines (from identical values up
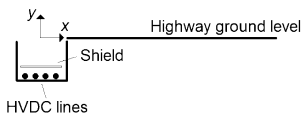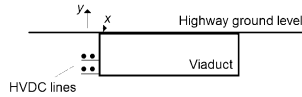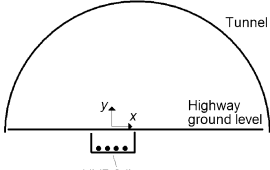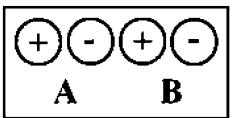
TABLE IV
LAYING CONFIGURATIONS

CONFIGURATION #1	
	Leading dimensions
	Laying depth: 130 cm
	Distance between cables: 21 cm
	Cable/shield distance: 40 cm
	Shield width: 70 cm
	Shield thickness: 0.6 cm
	Shield material: galvanized iron sheet
CONFIGURATION #2	
	Leading dimensions
	Line A height: - 70 cm
	Line B height: - 120 cm
	Distance between cables: 21 cm
	Shield is not present
CONFIGURATION #3	
	Leading dimensions
	Laying depth: 100 cm
	Distance between cables: 40 cm
	Shield is not present

TABLE V
CONDUCTOR DISPOSITIONS

Disposition	Electrical parameters
	r = 35.5 mΩ/km $l_{AA} = l_{BB}$ = 1.15 mH/km $l_{AB} = l_{BA}$ = -0.057 mH/km g = 1 nS/km c = 0.385 μF/km
	r = 35.5 mΩ/km $l_{AA} = l_{BB}$ = 1.15 mH/km $l_{AB} = l_{BA}$ = 0.057 mH/km g = 1 nS/km c = 0.385 μF/km

to the case where only one line is energized). Other harmonics, such as triplen and 6th, may arise under the assumption of non-idealities that have not been considered here.

The combination of all these factors in addition to the laying configurations and to the fact that the current amplitude is modified along the line length, produces a very high number of situations to be analyzed. Thus, a rational procedure has been adopted in order to simplify the analysis and individualize the most severe conditions for the magnetic-field levels around the cables.

V. RESULT DISCUSSION

A. Analysis of Configurations

The first step consists in defining the laying configuration and the conductor disposition which, for the same current value, produce the highest flux density levels around the line. For this purpose, 1-A current is imposed in the lines and the magnetic-field distributions for all laying configurations that are computed through the FEM/BEM code.

The results are summarized in Fig. 2(a)–(c) for laying configurations #1, #2, and #3, respectively, considering the case of both lines energized and the case when one line is out of service. The analysis shows that the field values produced in the highway laying are significantly lower with respect to those of the other configurations. Thus, laying configuration #1 can be disregarded when searching for the most severe conditions.

Moreover, the conductor disposition $(+-+-)$, which always gives rise to the highest field levels, is disadvantageous to be adopted and, when possible, should be replaced by the solution $(+--+)$.

A comparison between the remaining configurations shows that the most severe conditions are found in the viaduct (configuration #2) and in the tunnel (configuration #3). In the following text, taking into account the higher density of appliances, the tunnel laying will be used as a reference when evaluating the compliance with the ICNIRP and EMC standard field levels. It is important to note that the diagrams of Fig. 2 can also be employed to estimate the values of the static fields produced by the main dc component of the line current. In the rated conditions (dc current: 625 A), the maximum field level is ∼5.7 A/m, far lower with respect to the ICNIRP prescriptions.

B. Current Distribution Along the Line Length

The distribution of the amplitude of each current harmonic component along the line length is derived from the solution of the transmission-line equations. For this purpose, only the main laying (#1) is considered, taking into account that the other laying, of limited length, cannot significantly modify the line behavior. However, as reported before, the actual laying configuration becomes essential when computing a local magnetic-field distribution around the line in correspondence of a given point.

Some examples of current harmonic distributions along the line, computed for the two conductor dispositions and when only one line is energized, are presented in Fig. 3, showing the components with higher amplitude. In these cases, rated voltage vectors, without negative sequences, are imposed at the generator and user sides. The transmitted power is assumed to be equal to 80% of the rated one, as a conservative condition, because power reduction increases the harmonic content. Thanks to the assumption of equal firing angles, only harmonics of the $(12n)$th order are found, and the 12th one (600 Hz) usually prevails. However, the comparison between the three figures shows a strong increase of the 24th (1200 Hz) harmonic in the first conductor disposition. This behavior is caused by resonance phenomena, which depend on the geometrical characteristics of the lines and the conductor arrangement. The presence of harmonics in the supply obviously increases the risk of resonances which,
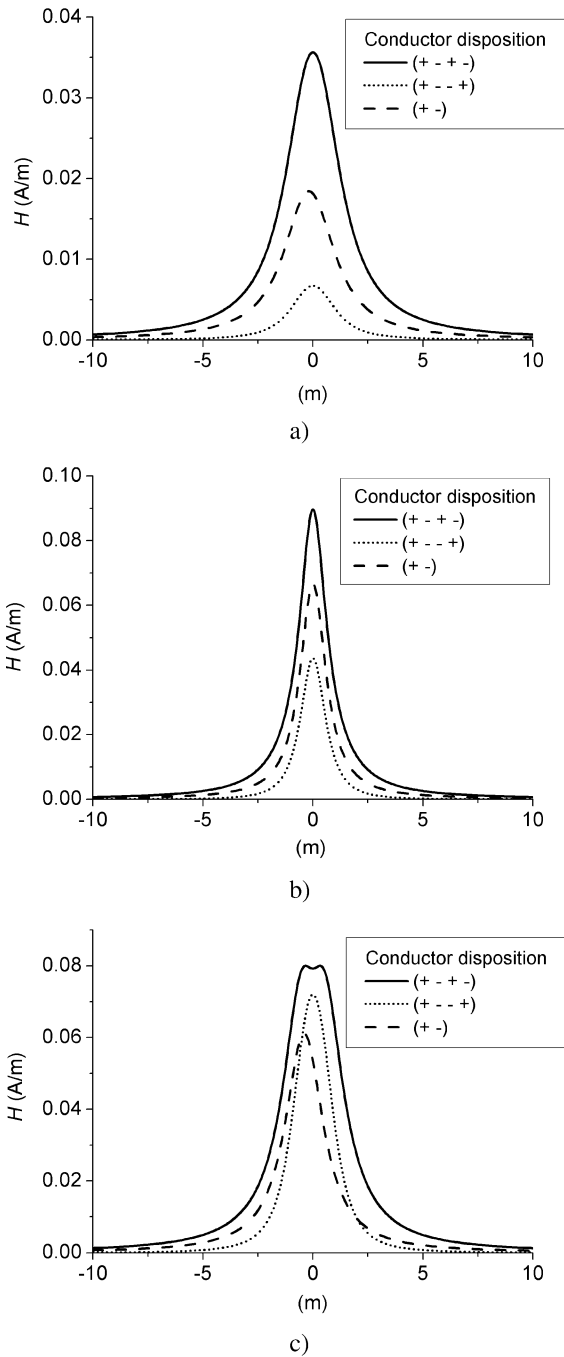
Fig. 2. Magnetic-field distribution along a horizontal line at the ground level, corresponding to a current of 1 A. The origin is placed at the system center. (a) Configuration #1 in the highway. (b) Configuration #2 in the viaduct. (c) Configuration #3 in the tunnel.
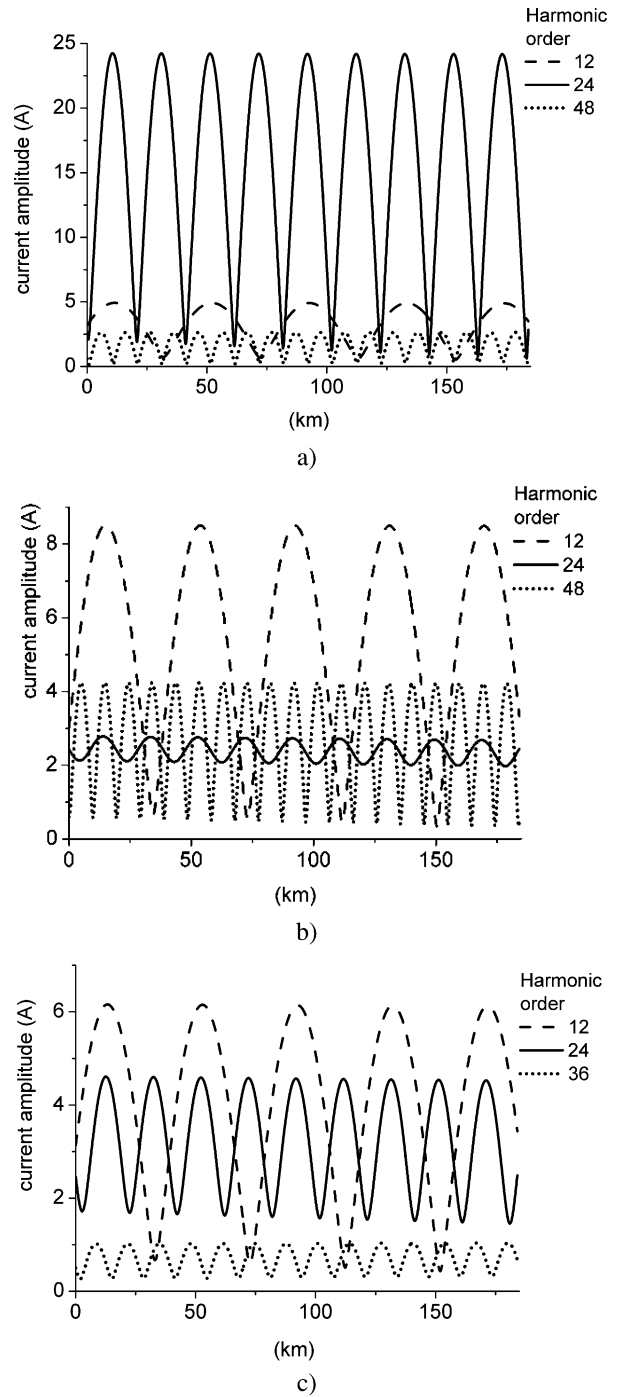

Fig. 3. Distribution along the line length of the amplitude (peak value) of the current harmonic components: (a) conductor disposition $(+ - + -)$, (b) conductor disposition $(+ - - +)$, and (c) only one line energized.

in turn, also affects the levels of the magnetic fields produced in the surrounding ambient.

C. Limits Evaluation Under the Rated Supply Conditions

In order to verify compliance with the EMC standard limits, a function $K_\mathrm{p}(y)$ is conveniently introduced, which describes the magnetic-field amplitude, generated by unitary currents (one for each supplied line), along a vertical line starting from the system center. Function $K_\mathrm{p}(y)$ is deduced for each laying by the same FEM/BEM solution previously adopted (see Subsection V-A).

The condition that must be verified to comply with the EMC standard limits is

$$I_n \cdot f_n < \frac{50}{K_p} \cdot H_\mathrm{lim}^{50} \qquad (1)$$

where n is the harmonic order, f_n is the corresponding frequency, I_n is the rms value of the nth harmonic component of the current, and H_lim^{50} is the EMC standard limit for magnetic field at 50 Hz presented in Table II (that is, 1 A/m for information-technology equipment; 3 A/m for residential, commercial,

and light industrial environments; and 30 A/m for heavy industrial environments). The values of I_n at any point of the line are deduced for a given laying configuration and conductor disposition from the diagrams of Fig. 3; in the following text, in order to guarantee conservative conditions, they will be assumed as the maximum value along the line for the considered harmonic component.

Condition (1) is expressed in a graphical form through the diagrams of Fig. 4, which refer to the tunnel laying (configuration #3). The intersection between the horizontal line (left-hand side of (1)), which depends on current amplitude and harmonic order, and the "limit curves," one for each considered limit at 50 Hz (expressing the right-hand side of (2)), determines the limit distance beyond which the EMC standards is satisfied for the considered harmonic component. Fig. 4 also reports the behavior of function $K_p(y)$. The quantities are evaluated under the same supply conditions of Fig. 3 (rated input and output voltages and 80% transmitted power), considering the two conductor dispositions [Fig. 4(a) and (b)] and when only one line is energized [Fig. 4(c)].

As an example, Fig. 4(a) shows that the 24th current harmonic complies with the EMC limit for information-technology equipment (1 A/m at 50 Hz) only at a distance grater than ~6 m from the conductors, while the limit corresponding to 30 A/m at 50 Hz is always satisfied. The comparison between the three figures again confirms that the first conductor arrangement $(+ - + -)$ gives rise to the highest magnetic fields in the environment and, when possible, should be replaced. In the other dispositions, the conditions are less severe and the EMC limits are always satisfied for a distance greater than ~ 1.5 m. All of the arrangements comply with the ICNIRP limits for general public exposure.

D. Limits Evaluation Under Any Supply Conditions

The investigations are performed also considering operating conditions different from the rated ones, where higher emissions could arise.

In a first example, the rated input and output voltages and 80% transmitted power are imposed, but a 2% negative sequence is added to the voltage vectors only on the generator side. The voltage unbalance also produces second-order harmonic (100 Hz) currents. The results are presented in Fig. 5, having assumed that only one line is energized. The current distribution along the line [Fig. 5(a)] puts in evidence of a large second-order component; however, its effects with respect to the EMC limits are very low [Fig. 5(b)] due to the reduced frequency value. Fig. 5(b) shows that, on the whole, this operating condition produces a magnetic field that is significantly lower than the ones under rated conditions.

More critical conditions are found when the voltage vectors at the generator and user sides are, respectively, 110% and 90% of the rated ones, while the transmitted power remains as 80% of the rated one. The results, obtained by supplying only one line and assuming that the negative sequence in the ac supply voltage is not present, are shown in Fig. 6. In particular, the current distribution along the line length [Fig. 6(a)] shows that the highest contribution is given by the 12th harmonic which, together with the 36th harmonic, also requires the greatest distance (about 2
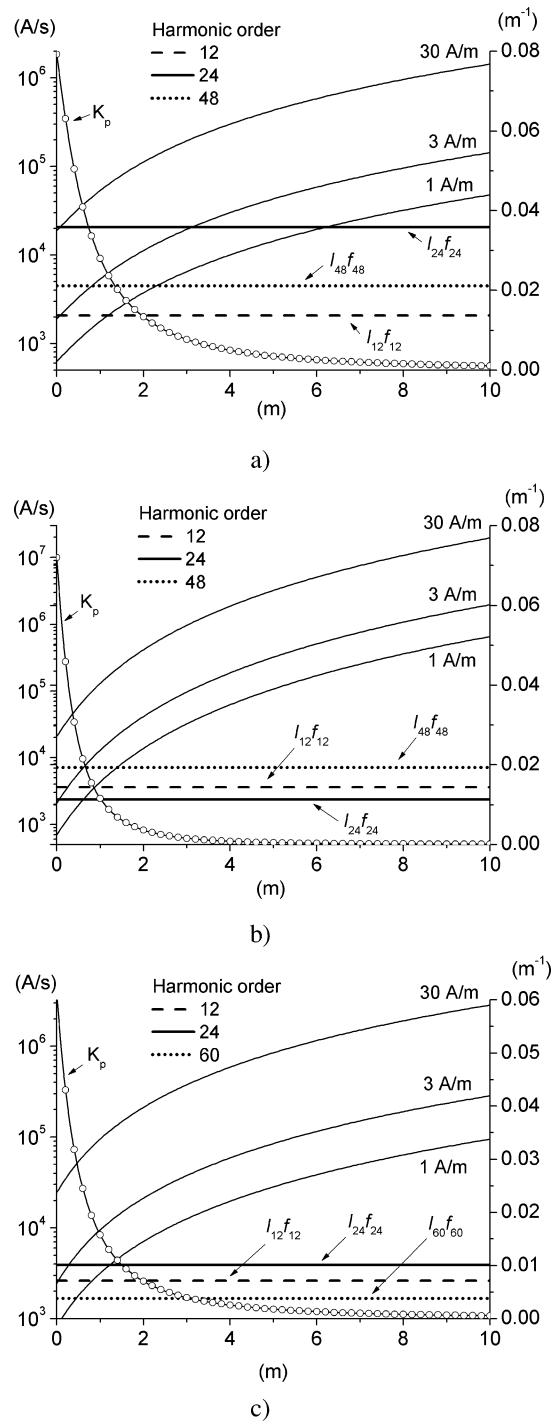

Fig. 4. Comparison between the magnetic field produced by each harmonic component of the current and the EMC limit curves. (a) Conductor disposition $(+ - + -)$. (b) Conductor disposition $(+ - - +)$. (c) Only one line energized. The scale of K_p is on the right axis.

m) from the system center in order to comply with the EMC standard limits.

The most critical conditions for the emissions are found when considering a conductor disposition $(+ - + -)$ having 80% transmitted power, 110% input voltage, 90% output voltage, and 2% negative sequence (with respect to the rated values). The corresponding diagrams of the current evolution along the line and of the comparison with the EMC limits are reported in Fig. 7(a)
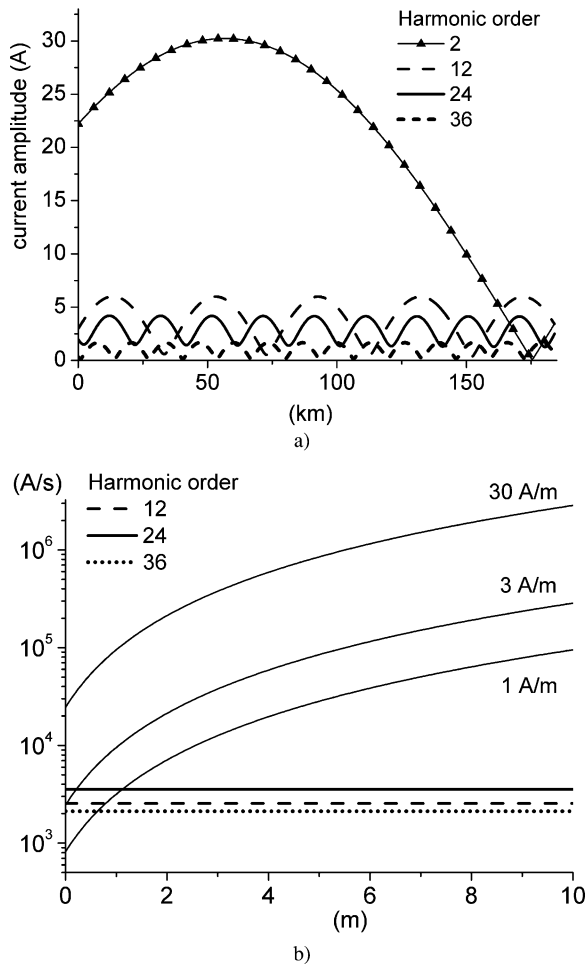
Fig. 5. Single line energized under rated input/output voltages with negative sequence. (a) Current distribution along the line. (b) Comparison of the EMC limits.

and (b), respectively. Here, the effects of the harmonics components (in particular of the 24th one) are significant and the distance for the EMC limits increases up to ∼ 5 m. This configuration, producing the highest magnetic fields in a large range of frequencies, has been taken as a reference in the successive study of possible alternative shielding solutions.

E. Shielding Solutions

In all of the cases previously analyzed, the field levels are lower than the ICNIRP limits for human exposure. Also, the EMC standard limits are, in general, verified at ground level. However, in some situations, as the one in Fig. 7, the magnetic-field values do not comply with the EMC standard limits, as shown in Fig. 8 which refers to the tunnel-laying configuration (configuration #3). Here, the three curves, respectively, for the 12th (600 Hz), 48th (2400 Hz), and 24th (1200 Hz) bound the region inside in which the magnetic field is higher than the EMC limit for information-technology equipment.

To limit this problem, accorded harmonic filters can be employed as is usually done with overhead HVDC lines. As an alternative, since EMC limits are overcome only in the tunnels that represent a limited portion of the HVDC line, localized shielding solutions can be conveniently adopted. In particular,
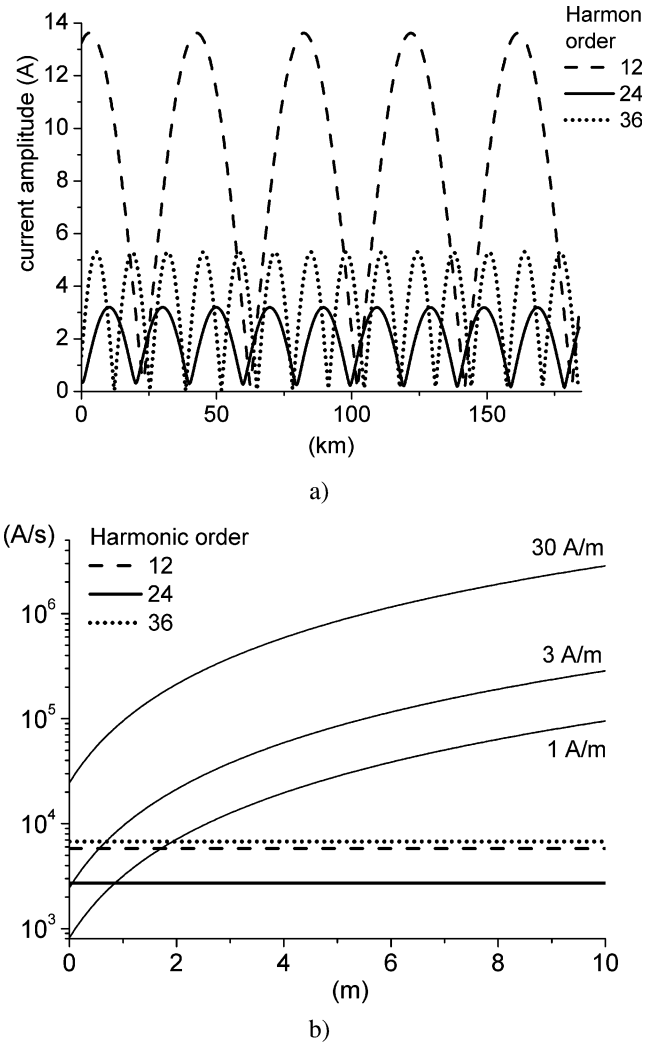

Fig. 6. Single line energized under 110% input voltage and 90% output voltage. (a) Current distribution along the line. (b) Comparison of the EMC limits.

two arrangements are considered here. The first shield consists of a simple plane aluminium sheet (electrical conductivity: 30 MS/m) having a thickness of 3 mm and width of 1.6 m. The shield is placed over the transmission line at a distance of 400 mm from its center. This solution gives rise to a limited reduction of the emissions in the environment, as shown in Fig. 9. The results are significantly improved when using two opposed U-shaped ferromagnetic laminations disposed to form a closed box, as proposed in [24]. The elements are constituted by zinked iron sheets (electrical conductivity: ∼6.5 MS/m, maximum relative permeability: ∼975) with a thickness of 3 mm, width of 1.6 m, and height of 400 mm. An airgap of 1 mm is imposed between the shields. The results, presented in Fig. 10, are evidence as to why the interference in the surrounding region is entirely avoided.

VI. CONCLUSION

This paper has been devoted to the analysis of the magnetic-field emissions of an HVDC transmission system, constituted by underground cables, with particular reference to the interconnection between Italy and France via the Frejus tunnel.
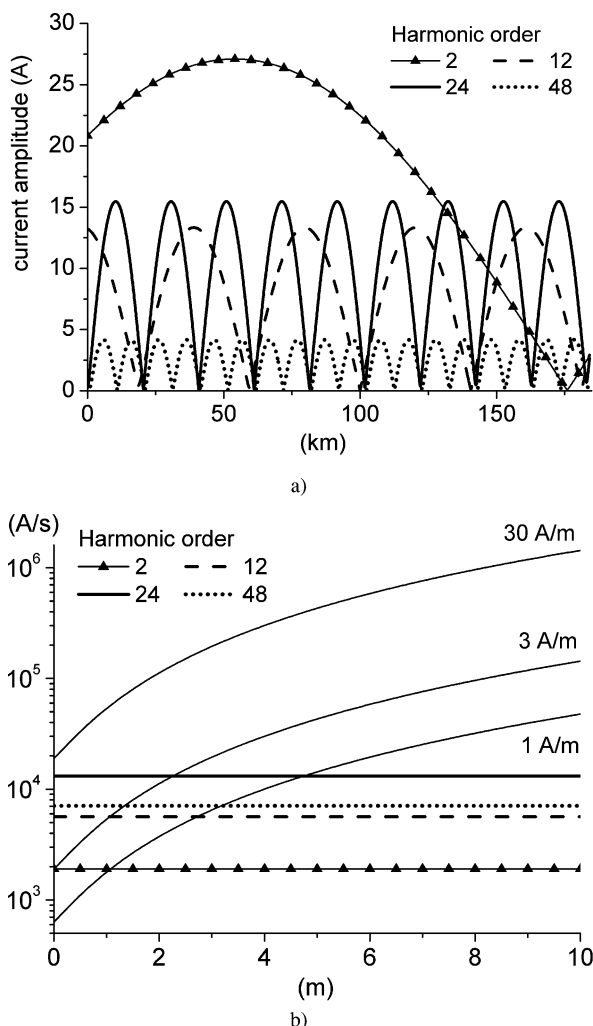
Fig. 7. $(+ - + -)$ conductor disposition under 110% input voltage and 90% output voltage: with a negative sequence (a) current distribution along the line and (b) comparison with the EMC limits.

Fig. 9. Bounds of the regions where the magnetic field is higher than the EMC limit for information-technology equipment considering the tunnel laying with a shield constituted by an aluminium sheet.

Fig. 10. Bounds of the regions where the magnetic field is higher than the EMC limit for information-technology equipment considering the tunnel laying with a shield composed of two opposed U-shaped ferromagnetic laminations.
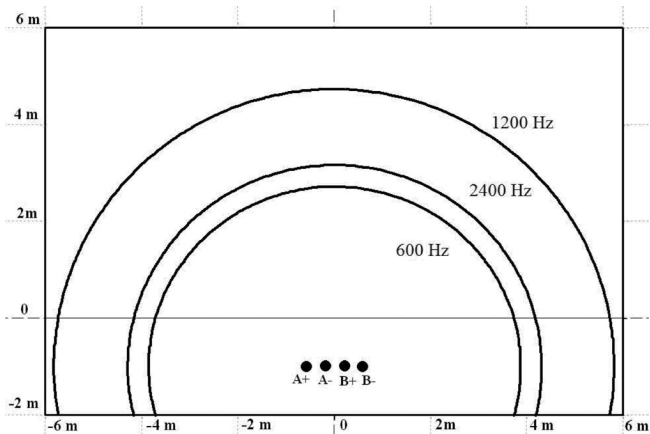

Fig. 8. Bounds of the regions where the magnetic field is higher than the EMC limit for information-technology equipment considering the tunnel laying without shield.

The analysis of the magnetic field produced by HVDC lines has been performed on different laying configurations and suppl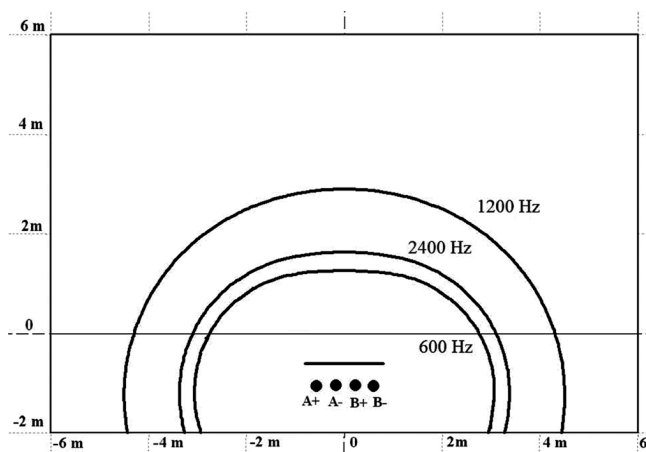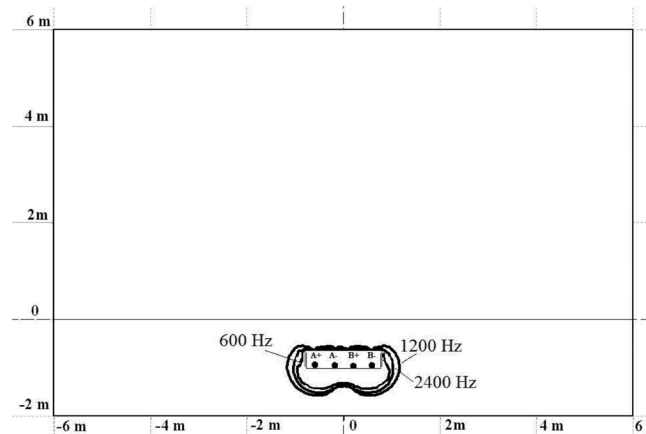y conditions through the use of different numerical methods. The results show that the magnetic field generated by the dc component of the currents is always significantly lower than the ICNIRP reference levels. Compliance with ICNIRP limits is also found for all of the harmonic components for general public and workers exposure. Concerning EMC problems, the analysis has shown that attention should be paid to the magnetic field generated by the higher order harmonic components mainly when resonance phenomena can significantly amplify the current amplitude. In this case, in order to limit the disturbances which could affect the electronic appliances depending on their immunity levels, some shielding solutions are proposed and discussed.

APPENDIX

The hybrid FEM/BEM formulation for computing the magnetic field generated by energized conductors, also with the presence of conductive/magnetic shields, is based on the concept of thin shell, that is, the dimensions of the open/closed shields are always prevalent with respect to their thickness [22]. This hypothesis is usually verified when considering power-line shielding.

Under this assumption, each 3-D shield is replaced by its 2-D surface, introducing interface conditions between the two opposite faces of the shell, to account for the electromagnetic phenomena within the material.

By denoting the two faces of the shield as (a) and (b), with a normal $\boldsymbol{n}$ oriented from (a) to (b), the following two interface equations arise:

$$
\begin{aligned}
&H_{m,n}^{(b)} + H_{m,n}^{(a)} + 2H_n^{(s)} \\
&\quad = \frac{j\zeta\sigma}{\omega\mu_o}\mathrm{div}_S\left[\frac{1}{\sigma}\left(\mathrm{grad}_S\phi^{(b)} - \mathrm{grad}_S\phi^{(a)}\right)\right]
\end{aligned}
\tag{A.1}
$$

$$
\begin{aligned}
&H_{m,n}^{(b)} - H_{m,n}^{(a)} \\
&\quad = -\frac{1}{\mu_o}\mathrm{div}_S\left[\eta^*\left(2\boldsymbol{H}^{(s)} + \mathrm{grad}_S\phi^{(a)} + \mathrm{grad}_S\phi^{(b)}\right)\right]
\end{aligned}
\tag{A.2}
$$

where $\boldsymbol{H}^{(s)}$ is the magnetic field generated by the sources (computed by the Biot–Savart law) and $\boldsymbol{H}_m$ is the reduced magnetic field, expressed through the gradient of a scalar potential ϕ, so that

$$
\boldsymbol{H} = \boldsymbol{H}_m + \boldsymbol{H}^{(s)} = \mathrm{grad}\phi + \boldsymbol{H}^{(s)}.
\tag{A.3}
$$

In (A.1) and (A.2), div_S and grad_S are, respectively, the surface divergence and gradient operators, μ_0 is the permeability of the air, coefficients ζ and η are defined as

$$
\zeta = \frac{\gamma}{\sigma tgh\left(\frac{\gamma d}{2}\right)} \quad \text{and} \quad \eta^* = \mu\frac{tgh\left(\frac{\gamma d}{2}\right)}{\gamma}
$$

where $\gamma = (1+j)/\delta$, δ is the penetration depth (at frequency f) of the shield of thickness d, the magnetic permeability is μ, and the electrical conductivity is σ

$$
\delta = \frac{1}{\sqrt{\pi f\mu\sigma}}.
$$

Equations (A.1) and (A.2) are solved through the FEM by applying the weak formulation and discretizing the shield surface in nodes/elements.

Two set of boundary-element equations are added to complete the system of equations, whose unknowns are the nodal values of reduced scalar potential ϕ and the normal component of the reduced magnetic field $H_{m,n}$ on both sides of the shield. The BEM equations, written for a closed shield discretized into M elements and separating region (a) and (b) are

$$
\begin{aligned}
\frac{1}{2}\tilde{\phi}_l^{(a)} = &+\sum_{j=1}^{M} H_{m,nj}^{(a)}\int_{\Omega_j}\Psi ds \\
&-\sum_{j=1}^{M}\int_{\Omega_j}\Phi^{(a)}(\nabla\Psi\cdot\mathbf{n}_j)ds
\end{aligned}
\tag{A.4}
$$

$$
\begin{aligned}
\frac{1}{2}\tilde{\phi}_l^{(b)} = &-\sum_{j=1}^{M} H_{m,nj}^{(b)}\int_{\Omega_j}\Psi ds \\
&+\sum_{j=1}^{M}\int_{\Omega_j}\Phi^{(b)}(\nabla\Psi\cdot\mathbf{n}_j)ds
\end{aligned}
\tag{A.5}
$$

where Ψ is the Green function.

This approach, described here for shields having linear magnetic properties, can be also generalized to nonlinear problems [25].

REFERENCES

[1] *"ICNIRP guidelines for limiting exposure to time-varying electric, magnetic, and electromagnetic fields (up to 300 GHz),"* 1998, ICNIRP Guidelines.

[2] *"ICNIRP guidelines on limits of exposure to static magnetic fields,"* 2009, ICNIRP Guidelines.

[3] EC Council recommendation on limitation of exposure of the general public to electromagnetic fields (0 Hz to 300 GHz), 1999, EC Council Recomm. 519.

[4] Directive 2004/40/EC of the European Parliament and of the Council of 29 April 2004 on the minimum health and safety requirements regarding the exposure of workers to the risks arising from physical agents (Electromagnetic Fields) (18th Individual Directive within the meaning of article 16(1) of directive 89/391/EEC), 2004.

[5] *IEC Electromagnetic Compatibility (EMC). Part 6-1: Generic Standards—Immunity for Residential, Commercial and Light-Industrial Environments, Part 6-2: Generic Standards—Immunity for Industrial Environments*, IEC Standard 61000-6, 2005.

[6] H. Zhao, H. Zhao, M. Zhao, and Y. Wang, "Computer simulation and measurements of HVDC harmonics," *Proc. Inst. Elect. Eng., Gen., Transm., Distrib.*, vol. 146, pp. 131–136, 1999.

[7] K. W. Louie, P. Wilson, R. W. Wachal, A. Wang, and P. Buchanan, "HVDC power system harmonic analysis in the time and frequency domains," in *Proc. Int. Conf. Power System Technology*, Chongqing, China, 2006, pp. 1–8.

[8] J. Liu, S. Fortin, H. Zhao, F. P. Dawalibi, and S. Tee, "Integrated computer approach to analyze the electromagnetic impact of transmission lines," in *Proc. Int. Conf. Power System Technology*, Chongqing, China, 2006, pp. 1–8.

[9] Z. Yu, J. He, B. Zhang, R. Zeng, S. Chen, J. Zhao, and Q. Wang, "Simulation analysis on radiated EMI from the DC buses in ± 500-kV HVDC converter stations," in *Proc. 18th Int. Zurich Symp. EMC*, Munich, Germany, 2007, pp. 357–360.

[10] Working Group 14.03.02, DC side harmonics and filtering in HVDC transmission systems, 1995, CIGRE brochure no. 92.

[11] *Guide for the Analysis and Definition of DC-Side Harmonic Performance of HVDC Transmission Systems*, IEEE Standard 1124-2003, 2003, pp. 1–68.

[12] "Italian law legge quadro sulla protezione dalle esposizioni a campi elettrici, magnetici ed elettromagnetici," Italian law N.36 2001.

[13] Italian DPCM fissazione dei limiti di esposizione, dei valori di attenzione e degli obiettivi di qualità per la protezione della popolazione dalle esposizioni ai campi elettrici e magnetici alla frequenza di rete (50 Hz) generati dagli elettrodotti. DPCM 08/07/2003.

[14] EN electromagnetic compatibility. electrical apparatus for the detection and measurement of combustible gases, toxic gases or oxygen. EN 50270:2006-11.

[15] *ECMA Limits and Methods of Measurement of Immunity Characteristics of Information Technology Equipment*, ECMA Standard 237, 1996.

[16] *EN alarm systems. Part 4: Electromagnetic compatibility. product family standard: Immunity requirements for components of fire, intruder and social alarm system*, EN 50130-4:1995-12.

[17] *EN electromagnetic compatibility—Road traffic signal systems—product standard*, EN 50293:2000-12.

[18] *EN uninterruptible power systems (UPS). Part 2: electromagnetic compatibility (EMC) requirements*, EN 62040-2:2006-03.

[19] *EN information technology equipment. Immunity characteristics. Limits and methods of measurement*, EN 55024:1998-09.

[20] O. Bottauscio, E. Carpaneto, M. Chiampi, D. Chiarabaglio, and I. Panaitescu, "Numerical and experimental evaluation of magnetic field generated by power busbar systems," *Proc. Inst. Elect. Eng., Gen. Transm. Distrib.*, vol. 143, pp. 455–460, 1996.

[21] M. Chiampi, G. Crotti, and D. Giordano, "Estimation of stray parameters of coils for reference magnetic field generation," *IEEE Trans. Magn.*, vol. 42, no. 4, pp. 1439–1442, Apr. 2006.

[22] O. Bottauscio, M. Chiampi, and A. Manzin, "Numerical analysis of magnetic shielding efficiency of multilayered screens," *IEEE Trans. Magn.*, vol. 40, no. 2, pp. 726–729, Mar. 2004.

[23] M. Borsero, G. Crotti, G. Vizio, and L. Zilberti, "Measurement of magnetic and electromagnetic fields in a HV AC/DC conversion substation," in *Proc. 16th Int. Symp. High Voltage Engineering*, Cape Town, South Africa, Aug. 2009, pp. 368–373.

[24] M. Zucca, G. Lorusso, F. Fiorillo, P. E. Roccato, and M. Annibale, "Highly efficient shielding of high-voltage underground power lines by pure iron screens," *J. Magn. Magn. Mat.*, vol. 320, pp. e1065–e1069, 2008.

[25] O. Bottauscio, M. Chiampi, and A. Manzin, "Nonlinear ferromagnetic shield modeling by the thin-shell approximation," *IEEE Trans. Magn.*, vol. 42, no. 10, pp. 3144–3146, Oct. 2006.

Luca Zilberti was born in Vercelli, Italy, in 1982. He received the B.S., M.S., and Ph.D. degrees in electrical engineering from the Politecnico di Torino, Turin, Italy, in 2004, 2006, and 2010, respectively.

Currently, he is in charge of a Research Grant at the Electromagnetism Division, Istituto Nazionale di Ricerca Metrologica (INRIM), Turin. His research activity is focused on the modeling of electromagnetic phenomena, with particular reference to the development of computational methods and their application to the analysis of human exposure to electromagnetic fields.

Enrico Pons received the M.Sc. degree in electrical engineering and Ph.D. degree in industrial safety and risk analysis from Politecnico di Torino, Turin, Italy, in 2004 and 2008, respectively.

Currently, he is a Postdoctoral Researcher at Politecnico di Torino. His research activities include power systems and electrical safety.

Oriano Bottauscio was born in Torino, Italy, in 1961. He received the degree in electrotechnical engineering from the Politecnico di Torino, Turin, Italy, in 1985.

Currently, he is a Senior Researcher within the Electromagnetics Division of the Istituto Nazionale di Ricerca Metrologica, Turin. He is the author/coauthor of many scientific papers. His research activity is focused on computational electromagnetics, with particular reference to the development of numerical methods and their application to the analysis of electromagnetic devices and magnetic material modeling.

Mario Chiampi received the degree in electrotechnical engineering from the Politecnico di Torino, Turin, Italy, in 1973.

From 1978 to 1987, he was a Research Scientist with the Istituto Elettrotecnico Nazionale Galileo Ferraris of Torino. Currently, he is a Full Professor of the fundamentals of electrical engineering with the Dipartimento di Ingegneria Elettrica, Politecnico di Torino. He is author/coauthor of many scientific papers. His research interests include numerical methods for electromagnetics, magnetic material modeling, and computer-aided design of electrical devices.

Michele Pastorelli was born in Novara, Italy, in 1962. He received the Laurea and Ph.D. degrees in electrical engineering from the Politecnico di Torino, Turin, Italy, in 1987 and 1992, respectively.

In 1988, he joined the Department of Electrical Engineering of the Politecnico di Torino, and since 2006, he has been Full Professor of Electrical Machines and Drives. He has authored many papers published in technical journals and conference proceedings. His research interests are in the field of power electronics, high-performance servo drives (both for industrial and commercial-residential applications), and energetic behaviors of electrical machines. He has been involved in research projects with industrial partners and in research activities funded by the Italian Ministry of Research and Innovation.

Dr. Pastorelli is a Registered Professional Engineer in Italy.